Unconditionally Stable Vector-based Meshless Method for Transient Electromagnetic Analysis

Sheyda Shams
MSc Student of Electrical Engineering
Electrical and Computer Engineering
Yazd University
Yazd, Iran, 89195-741
Email: sh.shams70@gmail.com

Ali Ghafoorzadeh yazdi
Ph.D., Assistant Professor
Electrical and Computer Engineering
Yazd University
Yazd, Iran, 89195-741
Email: aghafoorzadeh@yazd.ac.ir

Masoud Movahhedi
Ph.D., Assistant Professor
Electrical and Computer Engineering
Yazd University
Yazd, Iran, 89195-741
Email: movahhedi@yazd.ac.ir

Abstract— **In this paper, an unconditionally stable vector-based meshless method is presented. In the proposed method the leapfrog alternating-direction implicit (ADI) scheme is incorporated into a divergence-free vector RBF based meshless method. The vector RBF based meshless method has been recently proposed for numerical analysis. Unlike the scalar RBF meshless methods, this method has been proved to be divergence-free in the source-free regions. In conventional time-domain vector meshless method, the finite-difference scheme is used to approximate the time derivatives. Therefore, the CFL stability condition on the time-step limits the computational efficiency of the method. To overcome this limitation, in this paper, the ADI method is directly applied to the differential Maxwell's curl equations. Consequently, unconditional stability of the method is obtained by ADI technique and more accurate results are achieved by the use of vector basis functions. The effectiveness and efficiency of the proposed method are verified by a numerical example.**

Keywords- vector meshless method; divergence free; time-domain; alternating-direction implicit scheme

I. INTRODUCTION

For a long time, grid- or cell-based techniques, such as the finite-difference method (FDTD) [1], have been standard tools for numerically solving electromagnetic problems. However, some limitations of these methods such as difficulties in discretization scheme for problems with complex geometries still exist. Therefore, the need for the utilization of more powerful numerical techniques has laid the foundation for developing new numerical methods. Meshless methods, as one of these new methods, have attracted a great attention because of their capability in representing the problem domain and its boundary by using sets of nodes scattered in the problem domain and on its boundary [2]. Capability of solving problems without using connection information among nodes makes these methods suitable for modeling complex problems.

The radial basis function (RBF) method is an efficient meshless technique to solve partial differential equations. Moreover, this method has extended to transient electromagnetic field problems [3]. The meshless RBF method, despite its strengths, suffers from some limitations. One of these limitations is associated with divergence properties of electromagnetic fields. According to Maxwell's equations, in charge free regions electric and magnetic fields are always divergence-free. However, usually in the process of solving electromagnetic problems numerically, the obtained solutions are not divergence-free in the absence of source. This limitation has roots in the approximate nature of numerical techniques. Vector RBF, which is divergence free, was developed for non-electromagnetic problems in [4]-[5]. In addition, a matrix-valued divergence-free RBF was considered in [6], and its divergence-free property was proved theoretically. A meshless method incorporated with the vector RBF was first proposed for transient electromagnetic analysis in [7]. Results of this paper reveal that elimination of the artificial charges, which is obtained by the vector RBF, makes the numerical results more accurate. Consequently, the vector RBF meshless method because of its divergence-free property can be an efficient tool for solving time-domain electromagnetic problems more accurately.

In vector meshless method proposed in [7], an explicit finite-difference algorithm is used to approximate the time derivatives in Maxwell's equations. Therefore, a maximum time-step size is limited by the CFL stability condition. As a result, simulation time will be increased by choosing a small time-step and conditional stability can be seen. To overcome this problem, alternating-direction implicit (ADI) method can be applied for approximating time derivatives. The ADI method has previously been applied to several time-domain numerical methods. The 3D alternating-direction implicit finite-difference time-domain (ADI-FDTD) method was introduced in [8]. ADI formulation of the finite-element time-domain method is presented in [9]. Moreover, this method has been extended to meshless RPIM method in [10]-[11].

In this paper, we introduce an unconditionally stable vector meshless method by applying ADI scheme adopted from [12] to divergence-free vector RBF method. Formulation of the proposed method is presented. In addition, the stability and accuracy of the proposed method are investigated by a numerical example.

II. THE MESHLESS SCALAR RBF METHOD

In this section, we first give a brief description of the scalar RBF meshless method. A general function $u(\mathbf{x})$ at point $\mathbf{x}$ in scalar RBF meshless method can be interpolated by a

978-1-4673-8789-7/16/$31.00 ©2016 IEEE

combination of the function values at its surrounding nodes in computation domain Ω.

$$u(\mathbf{x}) = \sum_{j=1}^{N} a_j \phi(\|\mathbf{x}-\mathbf{x}_j\|), \quad \mathbf{x}, \mathbf{x}_j \in \Omega \tag{1}$$

Where $\phi(\|\mathbf{x}-\mathbf{x}_j\|)$ is the RBF and a_j are unknown coefficients to be computed. Gaussian form of the basis function is here [2]:

$$\phi_j = \phi(\|\mathbf{x}-\mathbf{x}_j\|) = e^{-\alpha|r/r_{\max}|^2} \tag{2}$$

where $r = \sqrt{(x-x_j)^2 + (y-y_i)^2}$, and (x_j, y_j) is the location of the jth node surrounding the point of interest at $\mathbf{x}$. By enforcing the function interpolation to pass through all the N nodes, unknown coefficients a_j can be obtained and finally field expansion (1) can be found. This method is applied to Maxwell's time-domain equations, and the time derivatives can be approximated by an explicit finite-difference scheme. Consequently, problems can be solved by using the obtained formulation for RBF meshless method.

III. VECTOR RBF MESHLESS METHOD

A. Vector Basis Function and Vector Shape Function

In this section we briefly refer to vector RBF meshless method formulation. The detailed analysis can be found in [7]. According to the paper, shape function for the vector RBF meshless method, based on the vector RBF proposed in [4]-[6] can be found as follows:

$$\mathbf{\Psi}_j = (-\Delta \mathrm{I} + \nabla\nabla^T)\phi_j \tag{3a}$$

$$\mathbf{\Phi} = \mathbf{B}_v \mathbf{A}_v^{-1} \mathbf{u}_s \tag{3b}$$

$$\mathbf{u} = \sum_{j=1}^{N} \mathbf{\Phi}_j \mathbf{u}_j \tag{3c}$$

where N is the number of scattered nodes in a local support domain, $\mathbf{u}_s = [\ldots \ u_{jx} \ u_{jy} \ u_{jz} \ \ldots]$, $\mathbf{B}_v$ includes vector RBFs, $\mathbf{u}_j = [u_{jx} \ u_{jy} \ u_{jz}]^T$ and

$$\mathbf{A}_v = \begin{bmatrix} \Psi(\|\mathbf{R}_1 - \mathbf{R}_1\|) & \Psi(\|\mathbf{R}_1 - \mathbf{R}_2\|) & \ldots & \Psi(\|\mathbf{R}_1 - \mathbf{R}_N\|) \\ \Psi(\|\mathbf{R}_2 - \mathbf{R}_1\|) & \Psi(\|\mathbf{R}_2 - \mathbf{R}_2\|) & \ldots & \Psi(\|\mathbf{R}_2 - \mathbf{R}_N\|) \\ \vdots & \vdots & & \vdots \\ \Psi(\|\mathbf{R}_N - \mathbf{R}_1\|) & \Psi(\|\mathbf{R}_N - \mathbf{R}_2\|) & \ldots & \Psi(\|\mathbf{R}_N - \mathbf{R}_N\|) \end{bmatrix}_{3N\times 3N}$$

B. Meshless Formulation

Electric and magnetic fields are expanded by using the obtained vector basis function and vector shape function. Finally, by considering Maxwell's equations without sources and applying central finite-difference scheme to time derivatives, the proposed meshless formulation can be obtained:

$$\mathbf{H}_i^{n+1/2} = \mathbf{H}_i^{n-1/2} - \frac{\Delta t}{\mu} \sum_{j}^{NE} \nabla \times \mathbf{\Phi}_j \mathbf{E}_j^n \tag{4a}$$

$$\mathbf{E}_i^{n+1} = \mathbf{E}_i^n + \frac{\Delta t}{\varepsilon} \sum_{j}^{NH} \nabla \times \mathbf{\Phi}_j \mathbf{H}_j^{n+1/2} \ . \tag{4b}$$

IV. ADI FORMULATION OF THE DIVERGENCE FREE MESHLESS METHOD

Now we present the numerical formulation of the ADI vector meshless method. In the conventional ADI scheme, one discrete time-step is broken up into two half time steps, and there is no time-step difference between electric and magnetic field components. S. J. Cooke et al. [12] introduced an alternative form for the ADI-FDTD scheme. In this algorithm, despite conventional ADI-FDTD scheme, the electric and the magnetic field terms are computed only at the half and at the full time-step, respectively. Therefore, this method reduces computational time in comparison to conventional ADI-FDTD scheme while they are algebraically equivalent.

In order to derive our formulation, we used the leapfrog ADI-FDTD formulation in [12] to obtain the following equations of the electric and magnetic vector fields:

$$\mathbf{E}^{n+1/2} - \frac{\Delta t^2}{4\mu\varepsilon}\left(\frac{\partial^2}{\partial y^2}\hat{a}_x + \frac{\partial^2}{\partial z^2}\hat{a}_y + \frac{\partial^2}{\partial x^2}\hat{a}_z\right) \bullet \mathbf{E}^{n+1/2} = \mathbf{E}^{n-1/2} - \frac{\Delta t^2}{4\mu\varepsilon}\left(\frac{\partial^2}{\partial y^2}\hat{a}_x + \frac{\partial^2}{\partial z^2}\hat{a}_y + \frac{\partial^2}{\partial x^2}\hat{a}_z\right) \bullet \mathbf{E}^{n-1/2} + \frac{\Delta t}{\varepsilon}\nabla \times \mathbf{H}^n \tag{5a}$$

$$\mathbf{H}^{n+1} - \frac{\Delta t^2}{4\mu\varepsilon}\left(\frac{\partial^2}{\partial y^2}\hat{a}_x + \frac{\partial^2}{\partial z^2}\hat{a}_y + \frac{\partial^2}{\partial x^2}\hat{a}_z\right) \bullet \mathbf{H}^{n+1} = \mathbf{H}^n - \frac{\Delta t^2}{4\mu\varepsilon}\left(\frac{\partial^2}{\partial y^2}\hat{a}_x + \frac{\partial^2}{\partial z^2}\hat{a}_y + \frac{\partial^2}{\partial x^2}\hat{a}_z\right) \bullet \mathbf{H}^n - \frac{\Delta t}{\mu}\nabla \times \mathbf{E}^{n+1/2}. \tag{5b}$$

We can approximate electric and magnetic fields by using vector shape functions as follows:

$$\mathbf{E} = \sum_{j}^{NE} \mathbf{\Phi}_j \mathbf{E}_j \tag{6a}$$

$$\mathbf{H} = \sum_{j}^{NH} \mathbf{\Phi}_j \mathbf{H}_j \tag{6b}$$

where *NE* and *NH* are the numbers of electric and magnetic field nodes respectively.

Here we consider (5), and substitute (6) into them. The following equations are obtained:

$$\sum_{j}^{NE}\mathbf{\Phi}_j\mathbf{E}_j^{n+1/2}-\frac{\Delta t^2}{4\mu\varepsilon}\left(\frac{\partial^2}{\partial y^2}\hat{a}_x+\frac{\partial^2}{\partial z^2}\hat{a}_y+\frac{\partial^2}{\partial x^2}\hat{a}_z\right)\bullet\sum_{j}^{NE}\mathbf{\Phi}_j\mathbf{E}_j^{n+1/2}$$
$$=\sum_{j}^{NE}\mathbf{\Phi}_j\mathbf{E}_j^{n-1/2}-\frac{\Delta t^2}{4\mu\varepsilon}\left(\frac{\partial^2}{\partial y^2}\hat{a}_x+\frac{\partial^2}{\partial z^2}\hat{a}_y+\frac{\partial^2}{\partial x^2}\hat{a}_z\right)\bullet\sum_{j}^{NE}\mathbf{\Phi}_j\mathbf{E}_j^{n-1/2}$$
$$+\frac{\Delta t}{\varepsilon}\nabla\times\sum_{j}^{NE}\mathbf{\Phi}_j\mathbf{H}_j^{n} \tag{7a}$$

$$\sum_{j}^{NH}\mathbf{\Phi}_j\mathbf{H}_j^{n+1}-\frac{\Delta t^2}{4\mu\varepsilon}\left(\frac{\partial^2}{\partial y^2}\hat{a}_x+\frac{\partial^2}{\partial z^2}\hat{a}_y+\frac{\partial^2}{\partial x^2}\hat{a}_z\right)\bullet\sum_{j}^{NH}\mathbf{\Phi}_j\mathbf{H}_j^{n+1}$$
$$=\sum_{j}^{NH}\mathbf{\Phi}_j\mathbf{H}_j^{n}-\frac{\Delta t^2}{4\mu\varepsilon}\left(\frac{\partial^2}{\partial y^2}\hat{a}_x+\frac{\partial^2}{\partial z^2}\hat{a}_y+\frac{\partial^2}{\partial x^2}\hat{a}_z\right)\bullet\sum_{j}^{NH}\mathbf{\Phi}_j\mathbf{H}_j^{n}$$
$$-\frac{\Delta t}{\mu}\nabla\times\sum_{j}^{NE}\mathbf{\Phi}_j\mathbf{E}_j^{n+1/2}. \tag{7b}$$

Finally, according to Kronecker's delta property of vector shape function, ADI formulation of the vector-based method can be obtained as:

$$\mathbf{E}_i^{n+1/2}-\frac{\Delta t^2}{4\mu\varepsilon}\sum_{j}^{NE}\left(\frac{\partial^2}{\partial y^2}\hat{a}_x+\frac{\partial^2}{\partial z^2}\hat{a}_y+\frac{\partial^2}{\partial x^2}\hat{a}_z\right)\bullet\mathbf{\Phi}_j\mathbf{E}_j^{n+1/2}=$$
$$\mathbf{E}_i^{n-1/2}-\frac{\Delta t^2}{4\mu\varepsilon}\sum_{j}^{NE}\left(\frac{\partial^2}{\partial y^2}\hat{a}_x+\frac{\partial^2}{\partial z^2}\hat{a}_y+\frac{\partial^2}{\partial x^2}\hat{a}_z\right)\bullet\mathbf{\Phi}_j\mathbf{E}_j^{n-1/2}$$
$$+\frac{\Delta t}{\varepsilon}\sum_{j}^{NH}\nabla\times\mathbf{\Phi}_j\mathbf{H}_j^{n} \tag{8a}$$

$$\mathbf{H}_i^{n+1}-\frac{\Delta t^2}{4\mu\varepsilon}\sum_{j}^{NH}\left(\frac{\partial^2}{\partial y^2}\hat{a}_x+\frac{\partial^2}{\partial z^2}\hat{a}_y+\frac{\partial^2}{\partial x^2}\hat{a}_z\right)\bullet\mathbf{\Phi}_j\mathbf{H}_j^{n+1}=$$
$$\mathbf{H}_i^{n}-\frac{\Delta t^2}{4\mu\varepsilon}\sum_{j}^{NH}\left(\frac{\partial^2}{\partial y^2}\hat{a}_x+\frac{\partial^2}{\partial z^2}\hat{a}_y+\frac{\partial^2}{\partial x^2}\hat{a}_z\right)\bullet\mathbf{\Phi}_j\mathbf{H}_j^{n}$$
$$-\frac{\Delta t}{\mu}\sum_{j}^{NE}\nabla\times\mathbf{\Phi}_j\mathbf{E}_j^{n+1/2}. \tag{8b}$$

V. Numerical Results

Here, to verify the stability and accuracy of the proposed ADI vector-based meshless method, a numerical example is presented. A 2-D lossless rectangular cavity with dimension 1.0 mm × 1.0 mm and perfectly conducting walls is considered. The problem domain is discretized with a set of electric field nodes and a set of magnetic field nodes. These nodes are arranged in such a way that each electric field node is surrounded by magnetic field nodes and vice versa. The modulated Gaussian pulse is used as the excitation current of the cavity and is specified as:

$$\mathrm{J}=A\cos(2\pi ft)\exp\left(-\left(\frac{t-t_0}{\tau}\right)^2\right)\hat{a}_x \tag{9}$$

where $A=1\times10^{10}$, $f=2.1\times10^{11}$, $t_0=16\times10^{-12}$ and $\tau=5\times10^{-12}$. The time variation of this pulse is shown in Fig. 1.

A. Verification of Stability

First, simulations were run for the problem with conventional vector based method and the maximum time-step which guarantees the stability of this method was determined, i.e., in this problem, $\Delta t_{MAX}=3.5\times10^{-13}$. Fig. 2 shows the electric field recorded inside the 2-D cavity with the vector based meshless method when $\Delta t=1.03\Delta t_{MAX}$. As can be observed, this method presents unstable solution when the time-step is a little larger than the stability limit. However, it is shown in Fig. 3 that the ADI vector meshless method remains with a stable solution even when the time-step is six times as large as the stability limit. The solutions were remained stable with even larger time-steps.

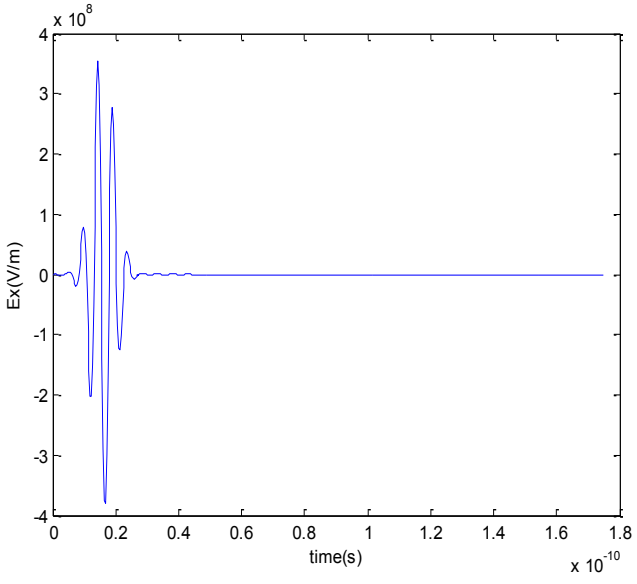

Figure 1. Time variation of the modulated Gaussian pulse excitation of the 2-D rectangular cavity.

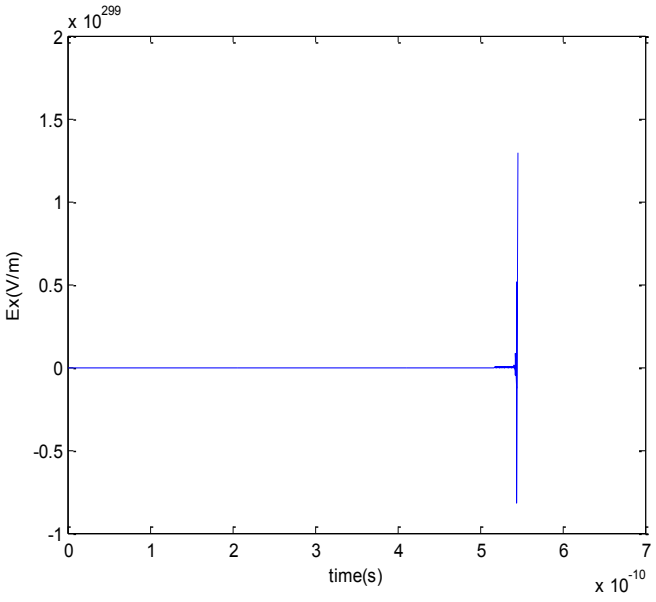

Figure 2. Ex field recorded at the observation point of the 2D resonator solved with the vector based meshless method $\Delta t = 1.03 \times \Delta t_{MAX}$.

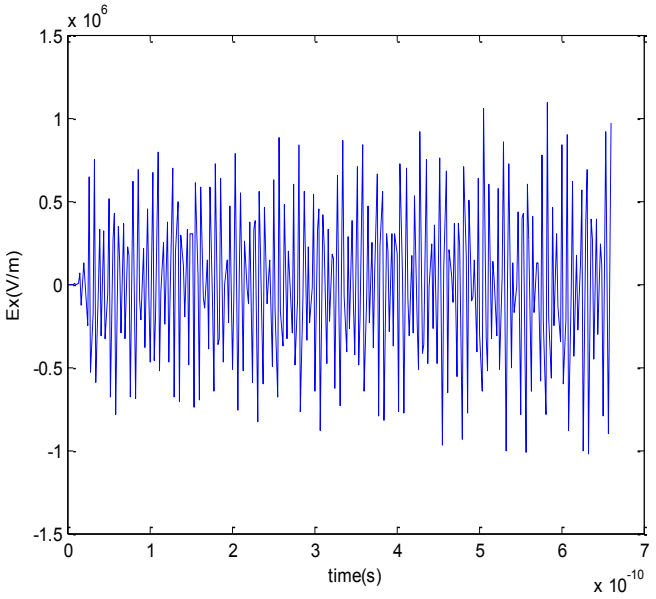

Figure 3. Ex field recorded at the observation point of the 2D resonator solved with the proposed ADI vector based meshless method $\Delta t = 6 \times \Delta t_{MAX}$.

B. Numerical Accuracy

The resonant frequencies were obtained through applying the Fourier transform on the time response. Table I lists the resonant frequencies in different time-steps for the TE_{10}^{z} mode as the dominant mode. The results show that, as expected, choosing a larger time-step increases the relative errors of the proposed ADI method. Moreover, in the proposed method we have to compute a matrix inversion. The computation of a matrix inversion would increase the load of calculations [13].

TABLE I. SIMULATION RESULTS WITH DIFFERENT TIME-STEP

Analytical Result (GHz)	**The proposed ADI vector meshless method**				**Conventional vector meshless method**	
	$\Delta t = 5\Delta t_{MAX}$		$\Delta t = 2\Delta t_{MAX}$		$\Delta t = \Delta t_{MAX}$	
	Result (GHz)	***Relative error***	***Result (GHz)***	***Relative error***	***Result (GHz)***	***Relative error***
149.89	155.8	3.94%	150	.07%	150.17	.18%

As a result, in the proposed scheme the number of time-steps will be reduced by increasing the time-step size at the cost of reasonable memory overhead.

VI. CONCLUSION

We introduced ADI formulation of vector meshless method in this paper. The proposed method increases the maximum time step size of the conventional vector-based meshless method. Therefore, this method can be assumed unconditionally stable. The number of time-steps will be reduced by increasing the time-step size at the cost of numerical errors and reasonable memory overhead.

REFERENCES

[1] A. Taflove, *Computational Electrodynamics: The Finite-DifferenceTime-Domain Method*. Norwood, MA, USA: Artech House, 1996.

[2] G. R. Liu and Y. T. Gu, *An Introduction to Meshfree Methods and Their Programming.* Springer: New York, 2005.

[3] S. J. Lai, B. Z. Wang, and Y. Duan, "Meshless Radial Basis Function Method for Transient Electromagnetic Computations," *IEEE Trans. Magn.,* vol. 44, no. 10, Oct. 2008.

[4] S. Lowitzsch, "Approximation and interpolation employing divergence-free radial basis functions with applications," Ph.D. dissertation, Dept. Math., Texas A&M Univ., College Station, TX, USA, 2002.

[5] C. P. McNally, "Divergence-free interpolation of vector fields from point values-exact $\nabla.B = 0$ in numerical simulations," *Month. Notices Roy. Astronom. Soc., Lett.*, vol. 413, no. 1, pp. L76–L80, Mar. 2011.

[6] S. Lowitzsch, "Matrix-valued radial basis functions: stability estimates and applications," *Adv. Comput. Math*., vol. 23, no. 3, pp. 299–315, Oct. 2005.

[7] S. Yang, Z. Chen,Y. Yu, and S. Ponomarenko, "A divergence free meshless method based on the vector basis function for transient electromagnetic analysis," *IEEE Trans. Micro. Theory Tech*., vol. 62, no. 7, pp. 1409–1415, Jul. 2014.

[8] T. Namiki, "The electromagnetic simulation system based on the FDTD mehod for practical use," presented at the Asia-Pacific Microwave Conf., Yokohoma, Japan, Dec. 1998.

[9] M. Movahhedi, A. Abdipour, A. Nentchev, M. Dehghan, and S. Selberherr, "Alternating-direction implicit formulation of the finite-element time-domain method," *IEEE Trans. Micro. Theory Tech*., vol. 55, no. 6, pp. 1322–1331, Jun. 2007.

[10] Y. Yu and Z. Chen, "Towards the development of an unconditionally stable time-domain meshless numerical method," *IEEE Trans. Micro. Theory Tech*., vol. 58, no. 3, pp. 578–586, Mar. 2010.

[11] Y. Yu and Z. Chen, "A hybrid ADI-RPIM scheme for efficient meshless modeling," *in Digests of IEEE MTT-S Int. Microw. Symp., Baltimore*, MD, USA, Jun. 5–10, 2011, pp. 1–4.

[12] S. J. Cooke, M. Botton, T. M. Antonsen, and B. Levush, "A Leapfrog Formulation of the 3D ADI-FDTD Algorithm," *Intl. Workshop on Computational Electromagnetics in Time-Domain*, Oct. 15-17, 2007, pp. 1-4.

[13] H. Razmjoo, M. Movahhedi, and A. Hakimi, "Electromagnetic time domain modeling using an improved meshless method," *in IEEE MTT-S International Microwave Symposium Digest*, 2011, pp. 1–4.